Laser-sustained plasma (LSP) nitriding of titanium

Kamat, Amar M.; Copley, Stephen M.; Segall, Albert E.; Todd, Judith A.

Published in:
Coatings

DOI:
10.3390/coatings9050283

Publication date:
2019

coatings

MDPI

Review

Laser-Sustained Plasma (LSP) Nitriding of Titanium: A Review

Amar M. Kamat [1,*], Stephen M. Copley [2,3], Albert E. Segall [2] and Judith A. Todd [2]

[1] Advanced Production Engineering Group, University of Groningen, Nijenborgh 4, 9747AG Groningen, The Netherlands

[2] Department of Engineering Science and Mechanics, Pennsylvania State University, 212 EES Bldg, University Park, PA 16802, USA; Stephen_Copley@comcast.net (S.M.C.); axs18@psu.edu (A.E.S.); jat20@psu.edu (J.A.T.)

[3] Applied Research Laboratory, P.O. Box 30, N. Atherton St, State College, PA 16804-0030, USA

* Correspondence: amar.kamat@outlook.com; Tel.: +31-64-149-0186

Received: 23 March 2019; Accepted: 24 April 2019; Published: 26 April 2019

Abstract: Titanium and its alloys possess several attractive properties that include a high strength-to-weight ratio, biocompatibility, and good corrosion resistance. However, due to their poor wear resistance, titanium components need to undergo surface hardening treatments before being used in applications involving high contact stresses. Laser nitriding is a thermochemical method of enhancing the surface hardness and wear resistance of titanium. This technique entails scanning the titanium substrate under a laser beam near its focal plane in the presence of nitrogen gas flow. At processing conditions characterized by low scan speeds, high laser powers, and small off-focal distances, a nitrogen plasma can be struck near the surface of the titanium substrate. When the substrate is removed, this plasma can be sustained indefinitely and away from any potentially interacting surfaces, by the laser power and a cascade ionization process. This paper presents a critical review of the literature pertaining to the laser nitriding of titanium in the presence of a laser-sustained plasma, with the ultimate objective of forming wide-area, deep, crack-free, wear-resistant nitrided cases on commercially pure titanium substrates.

Keywords: laser-sustained plasma; titanium; wear resistance; laser nitriding; case hardening

1. Titanium: Benefits and Drawbacks

Titanium and its alloys have been widely studied in the past few decades, mainly as potential replacements for steel, aluminum, and superalloys. Titanium possesses a high strength-to-weight ratio, is 40% less dense than steel and nickel-base superalloys, has a tensile strength higher than aluminum and comparable to martensitic stainless steel [1], and can withstand higher operating temperatures than aluminum [2]. Due to the formation of a thin, passive oxide on the surface, titanium has excellent corrosion resistance, making it a suitable candidate for harsh reactive environments [3] including the human body [4]. These properties have led to titanium being referred to as a "wonder metal" [5], with current and future applications in the aerospace, chemical, automotive, and biomedical industries, spurring recent research into titanium alloy development to achieve desired functionalities and properties [6–8]. However, the widespread use of titanium in the industry has been hampered by the high costs incurred during extraction, processing, and machining, making titanium more expensive than steel or aluminum [9]. Apart from this economic disadvantage, titanium suffers from a serious engineering drawback, namely, its poor tribological properties. Indeed, titanium is notorious for exhibiting high coefficients of friction and wear rates, as well as poor abrasion and fretting resistance when sliding against itself or other materials [10–13].

At room temperature, titanium has a hexagonal close-packed (hcp) crystal structure (known as α-Ti) with a *c*/*a* ratio of 1.587 that is less than the ideal value of 1.633 [14]. This makes titanium prone to slip along the prismatic $\{10\bar{1}0\}$ rather than the base plane {0001}, leading to an increase in friction coefficient [15] and galling tendency [14]. Titanium's metallic bond has a lower *d*-bond character compared to other transition metals, enhancing its surface chemical activity and increasing its tendency to form strong interfacial bonds with other mating surfaces. Buckley et al. [16] observed a relation between this low *d*-bond character of titanium and high coefficients of friction with itself and other materials. Miyoshi et al. [17] correlated the low theoretical tensile and shear strengths of titanium to high tendencies of material transfer and the resulting high friction coefficients; they reported friction coefficient values as high as 60 for titanium sliding against itself in a vacuum, making titanium especially vulnerable to galling and seizing [11]. Molinari et al. [18] provided a metallurgical basis for the low wear resistance of Ti-6Al-4V (henceforth Ti64) alloys. The researchers also recognized two distinct speed-dependent wear regimes: at high sliding speeds, the titanium alloy was found to wear by delamination attributed to the low plastic shear strength and low work hardening behavior of titanium; at low sliding speeds, surface oxides formed and were easily worn by spalling and microfragmentation, thus leading to oxidative wear [18]. The preceding discussion makes it clear that the surfaces of titanium components need to be modified to improve their wear resistance before they can be used in tribo-applications such as precision gears, orthopedic implants, bolts and fasteners, among others. This paper reviews the laser-sustained plasma (LSP) nitriding process and its potential to achieve deep-case hardening of titanium and is structured as follows: Section 2 discusses various surface hardening treatments that are commonly employed to enhance the tribological properties of titanium surfaces; Section 3 presents a detailed review of the laser nitriding process including the role of near-surface plasma as discussed in the literature spanning the past three decades; finally, Section 4 describes recent research conducted at the Pennsylvania State University to study the unique properties of a LSP and its effects on the laser nitriding process, followed by the development of a novel two-step "LSP nitriding-remelting" method to form homogenous, wide-area, deep, crack-free, and wear-resistant nitrided cases on commercially-pure titanium (CP-Ti) substrates.

2. Surface Hardening of Titanium

Surface engineering in tribology can be achieved using either surface coating or other modification techniques [19]. In surface coating methods, thin-film coatings of harder materials (such as TiN) are deposited on titanium to improve its wear resistance using techniques such as physical vapor deposition (PVD) and chemical vapor deposition (CVD) [20,21]. PVD processes further include ion plating, plasma spray, thermal evaporation, and sputtering [22]. Surface coating methods can achieve high hardness at the surface, but are characterized by low deposition rates, poor adhesion to the substrate (especially in evaporation processes), complex equipment, and low film thicknesses (1–10 μm) [23]; as such, PVD and CVD are incapable of producing a deep and hard case that is required in high contact stress tribosystems such as gears and bearings [20,24]. The surface hardness of titanium and its alloys can also be improved by forming thick-film coatings using laser cladding, wherein the desired coating in powder form (either preplaced on the substrate or made to flow through a nozzle) is melted and fused with the titanium substrate using a high-power laser [25–27], producing much thicker coatings than possible with PVD or CVD processes.

Surface modification of titanium can be implemented by thermochemical processes such as boronizing [28–30], carburizing [20], nitriding [24,31–40], and oxidizing [41–45]. Since the neutral atomic radii of the oxygen (0.6 Å), nitrogen (0.71 Å), and carbon (0.77 Å) atoms are about half or less than titanium (1.5 Å), O, N, and C atoms readily diffuse through the titanium lattice and can occupy the interstitial octahedral sites (0.61 Å radius) in the HCP structure of α-Ti [46]. The N and O atoms exhibit high interstitial solid solubility in the α-Ti phase, as seen in the phase diagrams of Figure 1 [47,48], causing a significant solid solution hardening effect [49]. Further, the interstitial O, N, and C atoms also increase the *c*/*a* ratio of the α-Ti HCP structure, which changes the slip plane from the prismatic

{10$\bar{1}$0} to the basal {0001} plane, increasing the galling resistance of titanium [15]. In addition, B, C, N, and O atoms also strengthen the titanium matrix by precipitation hardening, forming the hard ceramic phases TiB/TiB_2, TiC, TiN/Ti_2N, and TiO_2/TiO respectively within the titanium matrix. As nitrogen has the highest hardening effect of all these interstitial atoms [49], nitriding is a widely used and well-investigated thermochemical method of hardening titanium surfaces.

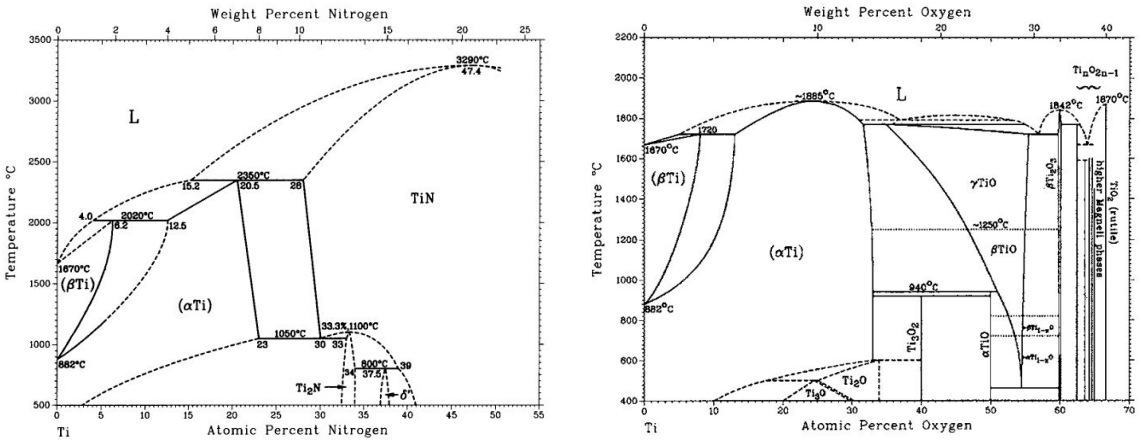

(**a**) (**b**)

Figure 1. (**a**) N-Ti and (**b**) O-Ti phase diagrams. Figure 1a reprinted with permission from Ref. [47] and Figure 1b with permission reprinted from Ref. [48]. Copyright 1987 Springer Nature.

Nitriding of titanium may be effected by ion implantation, diffusion, or laser/electron beam processes [20], each method differing in the mechanism of impregnating the titanium substrate with nitrogen. In ion implantation, nitrogen ions are accelerated into the titanium substrate through a voltage difference [20]; however, this method can only produce a compound nitride layer having a thickness of about 25–250 atomic layers [50]. As the name suggests, the diffusion method relies upon the diffusion of nitrogen atoms into the titanium surface at elevated temperatures. Nitrogen diffusion into the titanium substrate can be brought about either by heating the substrate to a high temperature in a nitrogen or ammonia gas atmosphere (gas nitriding) [31,33,34], or by exposing the substrate to a nitrogen plasma (plasma nitriding) that simultaneously heats the surface and provides nitrogen ions to it [36–39,51]. Plasma nitriding has the added advantage of an inherent sputtering phenomenon that also cleans the substrate and reduces impurities in the nitrided sample [51]. Both the gas and plasma nitriding processes are capable of forming functionally graded cases comprising a compound layer (TiN, Ti_2N) at the top and a diffusion zone containing a solid solution of nitrogen in titanium, α-Ti(N), deeper in the titanium substrate [21]. The hardness and depth of the resulting nitride cases depend upon the temperature and duration of the process; compound layer depths up to 50 µm (plasma nitriding) and 15 µm (gas nitriding) have been recorded, with total depths (including the diffusion layer) achieved up to 200–300 µm [31]. However, since diffusion takes place in the solid state, gas and plasma nitriding are slow processes, typically requiring 1–100 h [21]. Further, since the whole substrate experiences a high temperature (400–950 °C for plasma nitriding and 650–1000 °C for gas nitriding [21]) for long durations during the process, the bulk microstructure is affected along with the surface; thus, gas and plasma nitriding are not true "surface engineering" methods. Plasma and gas nitriding methods have also been found to reduce the fatigue strength of titanium alloys, especially at high processing temperatures [24]. Nitriding titanium using high energy density sources such as a laser circumvents these shortcomings while introducing new ones, as explained in Section 3. Figure 2 presents an overview of the various techniques used for surface hardening of titanium and its alloys, with a special focus on the nitriding of titanium, summarizing the discussion of Section 2.

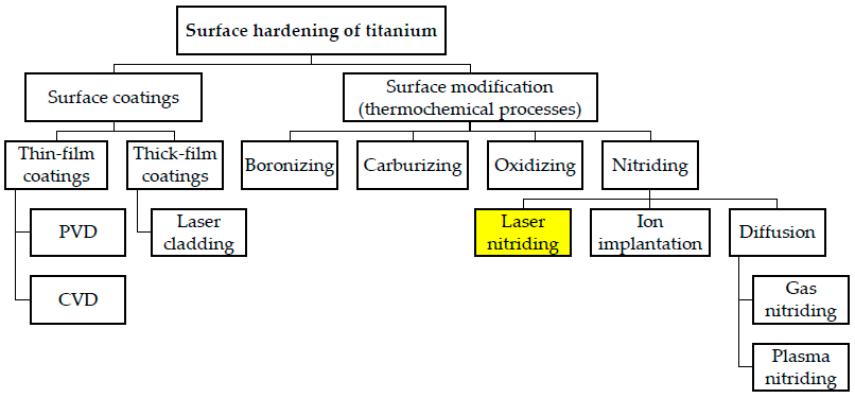

Figure 2. An overview of surface hardening methods for titanium and its alloys.

3. Laser Nitriding of Titanium

3.1. Background

Lasers are characterized by their monochromatic, coherent, polarized, narrow, and low-divergence beams. Focused laser beams can therefore deliver large quantities of energy (kilowatts) to a narrow spot (usually a fraction of a millimeter) on the surface of the substrate, leading to high energy intensities of the order of 10^{10}–10^{12} W/m^2 during welding (compared to 10^6–10^8 W/m^2 for flux-shielded or gas-shielded arcs [52]). Furthermore, this energy is absorbed within the first few atomic layers of the substrate, making the laser ideally and uniquely suited to surface engineering applications such as nitriding of titanium. Given these benefits, laser nitriding of titanium has been extensively researched for more than three decades. A typical laser nitriding process can be described as follows:

- The titanium substrate, usually in the form of a test coupon, is scanned under a laser beam in the presence of pure or diluted nitrogen gas flow (Figure 3a), where the distance of the focal plane from the substrate is dictated by the desired beam spot size (and hence incident energy density) on the substrate. The laser beam can be operated in the pulsed or continuous-wave (CW) mode. The nitrogen gas issues through a nozzle that is either coaxial (coaxial nozzle) or at an angle to the laser beam (side nozzle). The process is usually conducted in a controlled environment containing pure or diluted nitrogen to avoid oxidation of the titanium substrate.
- Due to the high energy density of the laser beam at or near focus, the irradiated area of the titanium substrate melts to a depth of hundreds of microns and incorporates nitrogen at its molten surface. The nitrogen-rich titanium melt is transported deeper into the melt pool by convection currents. The main driving mechanism for convection is the so-called Marangoni force arising out of surface tension gradients; since the surface tension for liquid titanium decreases with increasing temperature, the center region of the free surface of the melt pool has lower surface tension than at the edges, driving fluid flow from the center to the edges (Figure 3b). Since nitrogen transport by diffusion in the liquid phase is enhanced by convection, the laser nitriding process is much faster than solid-state diffusion processes such as gas nitriding and plasma nitriding.
- When the laser beam moves away from the area under consideration (e.g., Y-Y in Figure 3b) as the substrate is scanned, the nitrogen-rich melt experiences rapid and non-equilibrium solidification due to a "self-quenching" effect whereby the surface rapidly loses heat to the bulk via conduction. This results in the precipitation of phases such as stoichiometric or near-stoichiometric TiN, a solid solution of nitrogen in titanium, α-Ti(N), and martensitic titanium, α'-Ti. The TiN phase is gold-colored and hence easily identified on the surface of the treated sample. The TiN and α-Ti(N) phases form a strong metallurgical bond with the substrate, thereby enhancing the hardness and wear resistance of the treated substrate. The microstructure of the resulting nitrided layer can be controlled by varying processing parameters such as laser power, spot size (off-focal distance), scan speed, and the nitrogen gas flow rate. On the other hand, rapid solidification

makes the brittle nitrided layer susceptible to cracking and porosity, and causes an increase in surface roughness. Studies in the laser nitriding literature usually focus on overcoming these disadvantages (especially surface cracking) as detailed in Section 3.2.

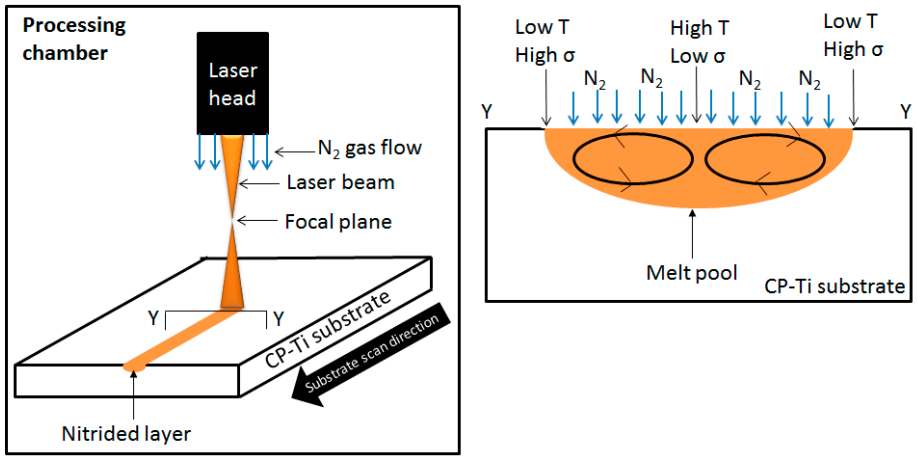

Figure 3. (**a**) Schematic of the laser nitriding process with coaxial nitrogen gas flow, and (**b**) convective transport of nitrogen in the melt pool at the transverse cross-section Y-Y. *T* and σ indicate temperature and surface tension respectively. CP-Ti denotes commercially-pure titanium.

3.2. Literature Review

3.2.1. Chronological Development of the Laser Nitriding Process

The use of lasers to nitride titanium and its alloys was first demonstrated in 1984 by Katayama et al. [53], who used pulsed and continuous-wave (CW) CO_2 and Nd:YAG lasers to harden the surface of titanium up to 700 HV (the Vickers hardness values of untreated CP-Ti and Ti64 alloys are 140–200 HV and 327–370 HV, respectively [1]). In the 1980's and 1990's, research focused on understanding and characterizing the laser nitriding process and finding optimal processing conditions to produce crack-free nitrided surfaces on CP-Ti and Ti64 substrates. Bell et al. [24] used the laser nitriding technique to improve the wear resistance and load bearing capacity of titanium for applications such as gears and bearings. Using a CO_2 laser in both the pulsed and CW modes, they were able to produce 500 µm deep nitrided cases on CP-Ti substrates. Two types of dendrites were observed in the microstructure: large dendrites near the surface, exhibiting cubic symmetry and hardness values close to 1500 HV and dendrites near the melted-unmelted region interface showing hexagonal symmetry and having a hardness of 600 HV. The cubic dendrites were identified as the compound TiN, while the hexagonal dendrites (which appeared to be hollow after deep etching) were identified as a solid solution of nitrogen in α-titanium, α-Ti(N). Morton et al. [54] reported an improvement in the wear behavior of laser-nitrided titanium during lubricated rolling and sliding at high Hertzian contact stresses; they used a CO_2 laser to nitride the Ti64 alloy using a side nozzle arrangement. Morton et al. [54] found that the angle of the nozzle needed to be at least 30° and that the nitrogen flow had to cover at least thrice the melt pool width to avoid oxygen contamination. They also reported that low scan speeds (less than 16 mm/s) led to embrittlement and high surface roughness, while high speeds (more than 48 mm/s) made the nitrided layer inhomogeneous. Diluting the nitrogen gas flow with argon (up to 60% dilution) and preheating the substrate up to 300 °C was found to reduce crack formation. No cracks were observed at surface hardness values of 600 HV or lower, although elsewhere [55] the threshold surface hardness value for crack formation was reported as 650 HV by the same authors. Roughness of the nitrided layer was attributed to the high viscosity of the TiN-rich melt, whereas the waviness was due to convective flow. Jianglong et al. [56] nitrided Ti64 using a

CO_2 laser and studied the general characteristics of the nitriding process. The authors noted that TiN formation depended upon a threshold energy density of 5×10^8 W/m^2, below which no nitride formation was observed irrespective of the scan speed. Given these observations, it was proposed that the mechanism listed below could help explain the laser nitriding process, where the [] refers to a melt and (N) represents the nitogen in the titanium structure [56]:

- Surface absorption $[Ti] + N_2 \rightarrow [Ti] + [N_2]$
- Nitrogen decomposition $[N_2] \rightarrow [2N]$
- Nitrogen transfer $[N]_{surface} \rightarrow [N]_{inside}$
- TiN precipitation $[Ti(N)] \rightarrow TiN + [Ti(N)]$
- Melt solidification $[Ti(N)] \rightarrow TiN + \alpha\text{-}Ti(N)$

According to Kloosterman et al. [57] who nitrided CP-Ti using a CO_2 laser in the presence of pure N_2 flow, the threshold laser energy density to form TiN was 2.5×10^9 W/m^2 or higher. They noted that apart from the mechanism proposed by Jianglong et al. [56], TiN could also form by the exothermic reaction $Ti + 0.5N_2 \rightarrow TiN$. Kloosterman et al. [57] further differentiated between two types of cracks in the nitrided layer: microcracks that were confined to the top 2–10 μm, and macrocracks that penetrated deeper into the solidified layer. The microstructure near the surface of the nitrided layer comprised a thin TiN layer (1–3 μm) and TiN dendrites that grew from the thin layer and were surrounded by nitrogen-rich Ti. Needle-like particles (560 HV hardness), coarse structures (300 HV hardness), and groups of TiN dendrites (swept away by convection currents) were observed by them deeper in the melt pool. Mridha and Baker [58] used a 1.35 kW CO_2 laser to nitride CP-Ti in a controlled pure-N_2 environment, and reported rippling, cracking, and pores at the surface; the cracks were seen to originate at the pores. The melt pool was inhomogeneous due to capillary flow of the melt. In a subsequent publication in which a parametric study of the process was conducted, Mridha and Baker [59] found that low gas flow rates and high speeds were essential to reduce surface crack formation on CP-Ti substrates in a pure-N_2 gas flow. Moreover, they reported that crack-free nitrided surfaces formed when the N_2 gas flow was diluted with either Ar or He gases. Although nitrogen dilution eliminated crack formation, the TiN dendrites produced by the pure N_2 flow were absent when the N_2 flow was diluted. The crack-free nitrided layers had depths up to 550 μm. Weerasinghe et al. [60] also found that diluting the nitrogen gas flow resulted in crack-free nitrided surfaces in CP-Ti substrates; however, the TiN dendrites were found to be confined to the top 25 μm of the solidified layer. Weerasinghe et al. [60] also explored the effects of a post-nitriding laser-remelting run in argon gas flow, and found that it increased the homogeneity and reduced the surface roughness of the nitrided layer. Hu and Baker [61] reported that the laser-nitrided Ti64 sample had a lower tendency to crack when preheated to about 300 °C (agreeing with Morton et al.'s [54] result) using a laser glazing run in argon gas flow. Xue et al. [62] found that preheating reduced the macrocracking tendency, while N_2 flow dilution eliminated microcracks on the surface of a pulsed Nd:YAG laser-nitrided Ti64 sample. Further, Xue et al. [63] measured residual stresses in the nitrided layer to be tensile (950 MPa in the scan direction and 800 MPa perpendicular to the scan direction); preheating reduced these tensile stresses and hence the tendency to form macrocracks. Xue et al. [63] also detected minor oxygen contamination on the nitrided surface (but none deeper in the nitrided layer), and concluded that oxidation did not contribute towards cracking.

Hu et al. [64] identified the "thick needle" phase (also referred to as "laths with rounded ends" [65], "plates" [66], or simply "dendrites" [67] in the laser nitriding literature) in laser-nitrided CP-Ti and Ti64 specimens as being hexagonal $TiN_{0.3}$. Xin et al. [65] analyzed the microstructure of Ti64 specimens nitrided using a CO_2 laser in an 80% N_2 flow and identified two distinct zones: zone I, about 50 μm from the surface, consisted of cubic $TiN_{0.8}$ dendrites, metastable hexagonal $TiN_{0.3}$, and martensitic α'-Ti; whereas zone II consisted primarily of nitrogen-rich martensitic α'-Ti. The atomic percentage of the nitrogen solute in the α'-Ti phase was found to be 3%–4% at the boundary of zones I and II, while it was less than 1% at the bottom of zone II. Nwobu et al. [67] used quantitative microanalysis to identify

two types of dendrites in the microstructure of nitrided CP-Ti: δ-TiN dendrites with nitrogen content greater than 30 at.%; and α-$TiN_{0.3}$ dendrites containing 18 at.%–22 at.% nitrogen, produced by the peritectic reaction L + δ-TiN → α (Figure 1a). Because of the measured composition of 18 at.%–22 at.%, they referred to this phase as α-$TiN_{0.25}$ instead of α-$TiN_{0.3}$. The effect of laser nitriding on the wear properties of titanium was studied by Yerramareddy and Bahadur [68], Xin et al. [69], Man et al. [70], and Ettaqi et al. [71], who reported an improvement in erosion and dry sliding wear resistance, abrasive resistance, cavitation erosion resistance, and a reduction in the coefficient of friction respectively.

In the 2000's, the process development of laser nitriding continued with a focus on reducing oxidation on the laser-nitrided surface and conducting wear resistance tests on the laser-nitrided titanium samples. Chen et al. [72] used a specially designed nozzle to avoid oxidation during pulsed Nd:YAG laser nitriding of Ti64 in an uncontrolled atmosphere. They concluded that oxygen-free nitriding was possible when the nitrogen gas flow was sufficiently low to maintain laminar flow conditions; high flow rates promoted oxygen contamination of the flow through turbulent mixing and led to oxide formation at the surface. Work by Abboud et al. [73] (who used a gas-shielding device to avoid oxidation during CO_2 laser nitriding of Ti64) and Chan et al. [74] (who investigated the extent of oxidation of CP-Ti and Ti64 during fiber laser nitriding in open atmosphere) agreed with Chen et al. [72] that turbulent gas flows should be avoided to ensure oxide-free nitrided layers. Raaif et al. [75] and Kaspar et al. [66] used a bell-shaped inert gas cover to maintain an oxygen-free atmosphere during CO_2 laser nitriding of CP-Ti and Ti64 respectively. More recently, Katahira et al. [76] successfully conducted pulsed laser nitriding on Ti64 in open atmosphere using a specially designed jig to prevent oxidation.

Several researchers also discussed the effect of the laser nitriding treatment on the wear and corrosion properties of titanium, the latter being especially important in biomedical applications where good corrosion fatigue resistance is required [77]. Geetha et al. [78], who nitrided the biomedical Ti-13Nb-13Zr alloy using a pulsed Nd:YAG laser and reported improved corrosion resistance compared to the base alloy, argued that the surface roughness inherent to the laser nitriding process (especially when carried out in a pure-N_2 environment) can be advantageous for osseointegration. Vadiraj et al. [79] nitrided a biomedical Ti alloy with a pulsed CO_2 laser and found a reduction in fretting wear rate. Sathish et al. [80], Zhang et al. [81], Majumdar [82], Dahotre et al. [83], Chan et al. [84], and Hussein et al. [85] also reported an improvement in the wear and corrosion resistance, as well as osseointegration of laser-nitrided biomedical titanium alloys. Kaspar et al. [66] used a CO_2 laser to nitride Ti64 in dilute N_2 environments and found that increasing the hardness to a value of 550 HV was enough to significantly increase the cavitation erosion wear resistance, which is important in applications such as pumps, impellers, and steam turbine blades. Recently, the use of Ti64 in automotive applications was explored by Duraiselvam et al. [86]. They used a CW diode laser with a rectangular beam profile to produce a 120 μm-thick nitrided layer with a hardness of 760 HV on Ti64 specimens; the nitrided sample performed better than grey cast iron at the same wear testing conditions, prompting the authors to patent their technique as a viable process of producing wear-resistant Ti64 specimens that can replace grey cast iron in disk brake rotor applications. Finally, Briguente et al. [87] also recently demonstrated an improvement in the creep resistance of Ti64 after a laser nitriding treatment, the first creep resistance test of its kind for laser-nitrided titanium alloys.

Apart from CO_2 and Nd:YAG lasers, researchers in recent times have also used free electron (FEL) [88,89], diode [82,86,90], and Ytterbium lasers [83] to perform nitriding of titanium. Lisiecki [90] lists higher absorption and more uniform heating as some of the main advantages of using a diode laser with a rectangular beam mode over more conventional laser sources such as the CO_2 laser with a Gaussian beam mode. Finally, two-dimensional (2D) finite element models of the heat and mass transfer occurring during laser nitriding were developed by Kuznetsov and Nagornova [91], Dahotre et al. [92], Xuan et al. [93], and Höche et al. [88]; while the first two papers neglected fluid flow, Höche et al. [88] considered both convection and diffusion in their model, and calculated several important dimensionless numbers such as the Peclet number (ratio of convective heat transfer to conductive heat transfer, value close to 10), Reynolds number (ratio of inertial forces to viscous forces,

value close to 500), and the Marangoni number (ratio of the Marangoni surface tension gradient forces to the viscous forces, value close to 5000) in the melt pool. Using their 2D model, Höche et al. [88] were able to predict surface deformation due to Marangoni flow, and recognized the tradeoff between high melt depths and low surface roughness, since the convective effects responsible for transporting nitrogen deeper into the melt pool were also responsible for deforming the surface and reducing surface quality.

3.2.2. Role of Near-Surface Plasma in Laser Nitriding of Titanium

If the laser energy density is high enough (of the order of 10^{10} W/m^2 [52]), the irradiated area of the substrate melts and vaporizes, leading to the formation of a plasma plume near the surface. A simplified description of the formation of such a laser-induced plasma is presented below [94]:

- In a metal where the first ionization potential is typically low, the metal vapor is easily ionized by the high intensity of the laser beam, giving rise to primary free electrons near the surface. Free electrons can also be generated by thermionic emission and the photoelectric effect [95].
- These primary free electrons gain energy by absorbing the laser radiation through a process called inverse bremsstrahlung. The energetic free electrons then collide with the neutral atoms and molecules of the processing gas, causing dissociation and ionization and producing secondary free electrons and ions in the process. This triggers a cascade ionization process in the gas, leading to gas breakdown and plasma formation. Gas breakdown is said to have occurred when the free electron density is of the order of 10^{24}/m^3 [96]. The presence of the primary free electrons reduces the threshold intensity required to cause optical breakdown of the processing gas by about four orders of magnitude [97], as well as the effective ionization potential of the processing gas [94]. According to Grigoryants [94], the threshold power density for a CO_2 laser to cause optical breakdown is approximately 6×10^9 W/m^2.
- The absorption of the laser energy by the plasma increases with the degree of ionization (i.e., the free electron density); if the laser is operated in the CW mode, a steady state can be reached when the absorbed laser energy is balanced by losses due to plasma re-radiation. In the steady state, the laser energy can sustain the plasma in a coaxial flow of the processing gas even when the original source of free electrons, the metal substrate, is removed from the laser beam path. Such a plasma has been referred to as a "continuous optical discharge" (COD) plasma [98] or a "laser-sustained plasma" (LSP) [99] in the literature; the latter terminology will be used in this paper.
- Peak temperatures in the range of 15000–17000 K have been measured at the core of steady-state argon LSP's [99,100]. Although it is more difficult to characterize a nitrogen LSP, its peak temperature is expected to be the same order of magnitude. This makes the LSP an interesting tool from the standpoint of high-temperature materials processing.

Although plasma formation is a commonly encountered phenomenon in laser materials processing [52,101], it has received limited attention in the laser nitriding literature. Morton et al. [54], probably drawing an analogy from laser welding processes, differentiated between two regimes of melting during laser nitriding: "normal melting" below laser power densities of 10^9 W/m^2 where energy transfer occurred through photons impinging upon the surface with an efficiency of less than 50%, and "keyhole melting" above power densities of 10^9 W/m^2 where plasma formation resulted in energy transfer efficiencies close to 100%. Although higher melt depths were achieved within the keyhole melting regime, it was fraught with problems such as high surface roughness, specimen distortion, and crack formation, and was thus deemed undesirable by the authors [54]. Thomann et al. [97] studied the laser-induced plasma that formed during pulsed CO_2 and XeCl laser nitriding of CP-Ti substrates; they found that the CO_2 laser-induced plasma occurred due to gas breakdown and was rich in ionic and atomic nitrogen species. The investigators also concluded that near-surface plasma formation enabled better energy coupling between the laser and the substrate and was hence necessary for the nitriding process [97]. Geetha et al. [78] observed near-surface plasma formation in their pulsed

Nd:YAG laser nitriding experiments in both pure and dilute nitrogen atmospheres; they noted that nitrogen dissociation in the plasma led to greater nitrogen diffusion rates into the melt pool. Moreover, the researchers reported that in an argon-diluted nitrogen atmosphere, ionic argon in the Ar-N_2 plasma hindered the diffusion of nitrogen, leading to a dendrite-free microstructure; as noted earlier, this effect has been observed before in the laser nitriding literature [59,60,69], albeit in the absence (or without the mention) of plasma formation. Höche et al. [102] and Ohtsu et al. [103] also argued that plasma formation aided the nitrogen dissociation process leading to the formation of nitrogen radicals that can diffuse faster into the titanium melt pool; plasma formation was thus dubbed beneficial to the laser nitriding process. Yu and Sun [104] conducted laser nitriding of titanium using a CO_2 laser in the presence and absence of a nitrogen plasma struck and sustained using an independent plasma gun. They found that at the same laser power density (10^9 W/m^2), the presence of the nitrogen plasma significantly enhanced the nitriding efficiency; this was attributed to the greater nitrogen intake occurring due to the presence of ionic and atomic nitrogen in the plasma.

On the other hand, Abboud et al. [73] took precautions to avoid plasma formation in their CO_2 laser nitriding experiments of Ti64, because the plasma (a) absorbed the laser radiation and hence reduced laser absorption on the titanium substrate, and (b) occasionally caused the focusing lens to break. Chen et al. [72] reported that the titanium-rich plasma pushed the nitrogen gas flow away from the titanium substrate and hence acted as a barrier between the nitrogen flow and the titanium substrate; consequently, they recommended that the laser power density be maintained at low values to prevent metal evaporation and subsequent plasma formation. However, Ohtsu et al. [105] found that the titanium-rich plasma could be confined to the substrate by maintaining a high enough pressure of nitrogen gas (100 kPa); at such high pressures, nitrogen radicals could effectively interact with the melt, leading to efficient coupling between the nitrogen gas flow and the substrate and, as a consequence, thicker nitrided layers. A recent study by Chan et al. [74] also proved that a stable, "low-brightness", laser-sustained plasma can improve the nitriding quality and reduce oxygen contamination, in contrast to a "high-brightness" plasma that can cause defects (cracks, craters, etc.) in the nitrided layer. A summary of commonly encountered issues, their causes, and proposed solutions in the laser nitriding literature can be found in Table 1.

Table 1. Summary of commonly encountered issues in laser nitriding of titanium.

Issue	Cause	Proposed Solutions	References
Crack formation in nitrided layer	Residual tensile stresses	Preheating titanium substrate	[54,61,62]
		Diluting nitrogen flow with argon	[54,59,60,62,66,73,75]
		Laser remelting [1]	[106]
Surface roughness and melt pool inhomogeneity	Marangoni convection	Low laser power, high scan speeds, nitrogen dilution with argon	[54,73,88]
		Laser remelting	[60,106]
Oxygen contamination of nitrided layer	High affinity of titanium to oxygen above 600 °C	Covering thrice the melt pool width with N_2 flow	[54]
		Controlled N_2 atmosphere	[56–58,60,61,73,75,107]
		Specially designed gas flow devices, avoid turbulent flow	[66,72–76]
		Nitriding in the presence of plasma [1]	[104,108–110]
Plasma formation during nitriding	Cascade ionization due to high laser energy density	To be avoided (energy attenuation to substrate, risk of lens breakage, insufficient contact between titanium substrate and nitrogen gas flow)	[54,72,73]
		To be encouraged (better energy coupling between substrate and laser, higher diffusion rates of nitrogen in melt pool, enhanced nitriding efficiency, reduced surface oxidation [1])	[74,97,102,103,105,108–110]

[1] See Section 4 for more details.

4. Laser-sustained Plasma (LSP) Nitriding of Titanium

4.1. Background

The role played by near-surface plasma during CW CO_2 laser nitriding of commercially pure titanium (CP-Ti) was investigated in great detail in the Center for Multi-scale Wave-Material Interaction (CMWMI) at the Pennsylvania State University [100,106,108–112] in recent years, resulting in the development of the so-called "LSP nitriding" process that was capable of improving the wear resistance of CP-Ti in open and uncontrolled atmosphere with minimal surface oxidation. Using a combination of charge-couple device (CCD) imaging and optical spectroscopy, Nassar et al. [108] characterized the near-surface plasma formed during the laser nitriding process as a function of scanning speed and off-focal distance (OFD). They found three main processing regimes pertinent to plasma formation:

- At low scanning speeds and small OFD's (i.e., conditions favoring higher power densities and longer beam-substrate interaction times), a Ti-rich plasma formed near the surface and did not allow the nitrogen gas flow to interact with the substrate, resulting in surface oxidation (e.g., Figure 4, left); Chen et al. [72] made a similar observation and argued against plasma formation since they believed that the Ti-rich plasma baffled the contact between nitrogen and the titanium substrate.
- At higher scan speeds and larger OFD's, the near-surface plasma became richer in nitrogen species such as N and N^+; this ensured sufficient interaction between the gas and the substrate and resulted in near-stoichiometric golden-colored titanium nitride layers on the substrate (e.g., Figure 4, middle). This regime can be thought of as similar to the one studied by researchers such as Thomann et al. [97] who concluded that plasma formation was necessary for efficient laser nitriding, as mentioned earlier in Section 3.2.2.
- Finally, at high scan speeds and/or large OFD's, near-surface titanium plasma was not observed.

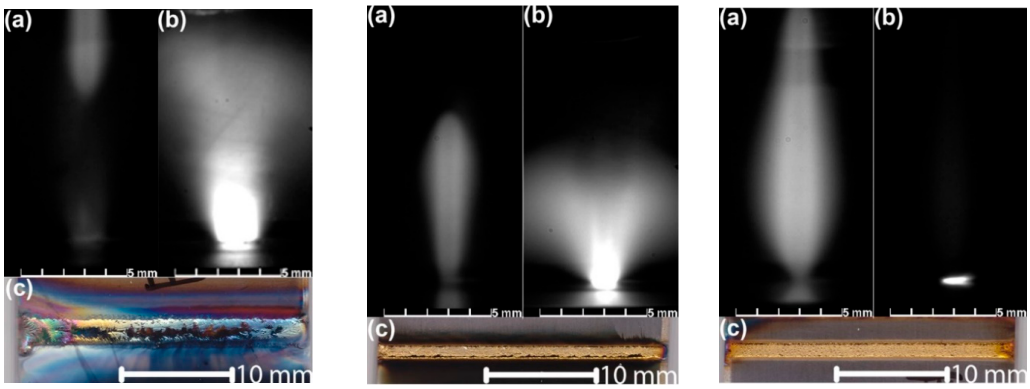

Regime 1
(8 mm OFD, 10 mm/s speed)

Regime 2
(4 mm OFD, 90 mm/s speed)

Regime 3
(8 mm OFD, 90 mm/s speed)

Figure 4. (**a**) Atomic nitrogen species (CCD image), (**b**) atomic titanium species (CCD image), and (**c**) photograph of the top surface of nitrided trail shown for Regime 1 (left), Regime 2 (middle), and Regime 3 (right) during LSP nitriding. Reprinted with permission from Ref. [108]. Copyright 2012 IOP Publishing.

Nassar et al. [108] thus found a processing window of scan speeds and OFD's (Regime 2) where a nitrogen-rich near-surface plasma struck during laser nitriding CP-Ti. Further, using X-ray photoelectron spectroscopy (XPS), Nassar et al. [108] observed that nitriding in the presence of nitrogen-rich plasma (Regime 2) in an open and uncontrolled atmosphere reduced surface oxidation in the nitrided layers, which was attributed to the gettering action of the plasma whereby the active nitrogen species reacted with atmospheric oxygen. Additionally, microstructural characterization of

the nitrided layers revealed no evidence of energy attenuation of the laser beam in the presence of plasma (Figure 5a,b); this was because the laser energy absorbed by the LSP was transferred to the substrate via two mechanisms: (a) energetic nitrogen species in the plasma colliding with the substrate, and (b) low-wavelength ultraviolet re-radiation by the LSP that is absorbed more efficiently by the titanium substrate compared to the CO_2 laser radiation (10.64 μm wavelength) [108]. The presence of nitrogen-rich plasma was thus found to be beneficial for the laser nitriding process.

Furthermore, to reap the benefits of nitriding in the presence of nitrogen-rich plasma beyond the processing conditions of Regime 2, Nassar et al. [108] also conducted nitriding experiments in the presence of a pre-struck laser-sustained plasma (LSP) in coaxial nitrogen gas flow. Laser-sustained plasma (LSP) is plasma that is generated and sustained near the focal plane of a laser beam in a gaseous atmosphere away from any potentially interacting surface. A freestanding nitrogen LSP had a tear-drop shape with dimensions of approximately 15 mm in the axial direction and 5 mm in the radial direction (Figure 6b). This approach, henceforth referred to as LSP nitriding, allowed the investigators to access the high scan speed/large OFD processing conditions of Regime 3 (Figure 4, right) in the presence of nitrogen-rich plasma. Nassar et al. [108] thus developed the LSP nitriding method that enabled laser nitriding of CP-Ti in open and uncontrolled atmosphere in the presence of nitrogen-rich plasma over a broad processing window of scan speeds and OFD's (Regimes 2 and 3 in Figure 5c).

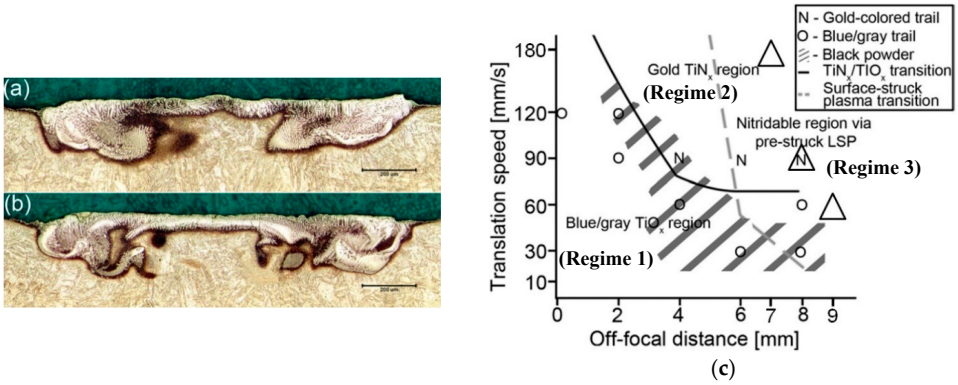

Figure 5. Optical micrograph of transverse cross-section of titanium nitrided (**a**) using a LSP, and (**b**) without a LSP (i.e., only the laser beam) at otherwise identical processing conditions; (**c**) processing window of Nassar et al. [108] showing different regimes during LSP nitriding of pure titanium, where the triangles represent processing conditions used by Kamat et al. [109] to compare laser nitriding in the presence and absence of the nitrogen LSP. The scale bars in (**a**,**b**) read 200 μm. Reprinted with permission from Ref. [108]. Copyright 2012 IOP Publishing.

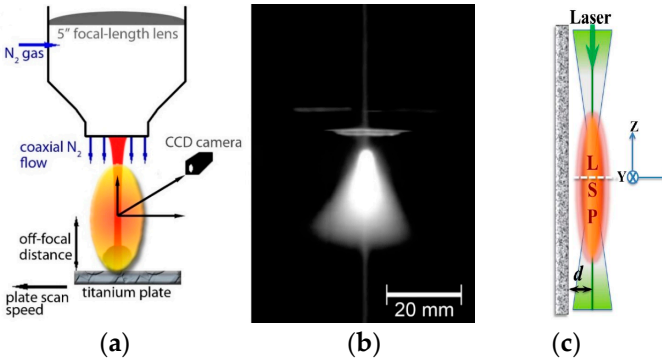

Figure 6. (**a**) Schematic of Nassar et al.'s [108] LSP nitriding process with the substrate perpendicular to the laser beam, (**b**) CCD image of freestanding nitrogen LSP, and (**c**) schematic of Black et al.'s [111] LSP nitriding process with the substrate parallel to the laser beam. Figure 6a,b reprinted with permission from Ref. [108]. Copyright 2012 IOP Publishing. Figure 6c reprinted with permission from Ref. [111]. Copyright 2017 Elsevier.

4.2. Effect of Nitrogen LSP on Heat and Mass Transfer During Nitriding

Black et al. [111] studied the interaction between a nitrogen LSP and a CP-Ti substrate by orienting the CP-Ti substrate parallel to the axis of the CO_2 laser beam (Figure 6c); these experiments differed from Nassar et al.'s [108] research (Figure 6a) where the substrate was normal to the laser beam. In Black et al.'s [111] configuration, the nitrogen LSP (Figure 6b) was the sole heating source since the laser beam did not irradiate the substrate, thus allowing them to isolate and study the interaction of the nitrogen LSP with the CP-Ti substrate. When the axis of the parallel nitrogen LSP was brought within 2–2.5 mm of the CP-Ti substrate and maintained there for 5 s, the substrate melted and incorporated nitrogen from the plasma, resulting in the synthesis of TiN layers up to 300 µm in thickness on the substrate with compositional gradation of nitride concentration (Figure 7a) and faceted crystal growth on the surface (Figure 7b). Such rapid growth of TiN crystals on the CP-Ti substrate without any direct radiation from the CO_2 laser beam demonstrated the utility of the nitrogen LSP as a high-energy source of active nitrogen species.

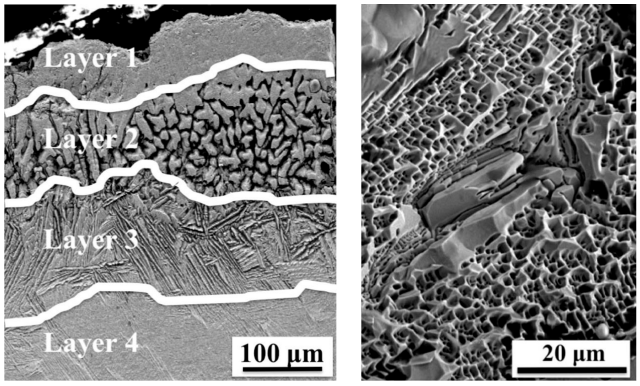

(**a**) (**b**)

Figure 7. SEM images of the titanium substrate nitrided in the parallel configuration (Figure 6c) showing: (**a**) longitudinal cross-section having four distinct layers of the nitrided titanium substrate, and (**b**) faceted crystal growth at the nitrided surface. Reprinted with permission from Ref. [111]. Copyright 2017 Elsevier.

To study the effects of the nitrogen LSP on heat transfer to the substrate, the temperature of the CP-Ti substrate (3.175 mm thick) was measured in both Nassar et al.'s perpendicular (Figure 6a) [109] and Black et al.'s parallel (Figure 6c) [113] configurations using K-type thermocouples welded to the back of the substrate. In the perpendicular configuration, Kamat et al. [109] conducted nitriding experiments in the presence and absence of a nitrogen LSP (i.e., LSP nitriding and conventional laser nitriding, respectively) and found that at similar processing conditions (8 mm OFD and 90 mm/s scan speed), the peak temperatures measured by a thermocouple located directly beneath the laser trail (on the backside of the CP-Ti coupon) were similar in both cases; moreover, the peak temperature recorded by a thermocouple located 13 mm away from the laser trail (again, on the back face of the substrate) was higher in the presence of the LSP. These observations suggested that the nitrogen LSP broadened the energy distribution incident upon the substrate without attenuating energy incident upon it. In the parallel configuration [113], two thermocouples were attached to the back face of the substrate (3.175 mm thick) so that the first (TC1) was directly horizontal with respect to the laser focal point while the second (TC2) was 10 mm below the first one; the nitrogen LSP was maintained at a distance d from the substrate for 5 s, where d was varied from 5 to 15 mm (Figure 8a). As seen in Figure 8b, the thermocouple TC1 located at the back of the substrate recorded a temperature rise of close to 500 °C after five seconds; treating the nitrogen LSP as a radiating sphere, using appropriate radiation view factors for the sphere-rectangle geometry, and using the lumped heat capacitance assumption for the titanium substrate for $d \geq 9$ mm (i.e., when the substrate could be assumed to be at a uniform temperature as seen in Figure 8b), Kamat [113] modeled the transient heat transfer

between the LSP and the substrate and estimated that the nitrogen LSP was equivalent to a heat source of 998 Watts within an error bar of ±10% for a laser power of 3.5 kW. Since calorimetric measurements showed that the nitrogen LSP absorbed about 38% (1.33 kW) of the 3.5 kW laser power sustaining it, it was concluded that the LSP re-radiated close to 75% of the power it absorbed from the laser, with the remaining 25% power used for heating the nitrogen gas exiting the LSP. Further, the presence of LSP was also found to increase the width of the nitrided trails and to reduce surface oxidation [109].

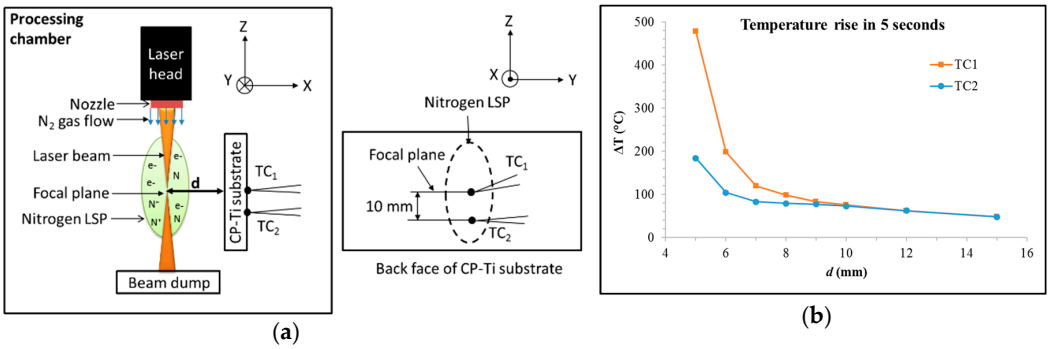

Figure 8. (**a**) Schematic of temperature measurement in parallel configuration with location of the thermocouples; (**b**) temperature rise, ΔT (°C), recorded by two thermocouples TC_1 and TC_2 at the end of 5 s.

To quantify the effect of the LSP on nitrogen intake into the melt pool, Kamat et al. [109] measured the weight increase of the titanium coupons after nitriding in the presence and absence of a nitrogen LSP, i.e., during LSP and conventional laser nitriding, respectively; the processing conditions (laser power, scan speed, OFD) were maintained the same to ensure a fair comparison. It was found that the nitrogen uptake was consistently higher in the case of LSP nitriding for all the tested conditions; a microstructural examination of the top surface of the nitrided layers indicated that LSP nitriding produced a more porous surface consisting of "expulsion sites" that were absent in conventional laser nitriding (Figure 9). The pore formation was attributed to oversaturation of molten titanium with energetic nitrogen species from the plasma, wherein the excess nitrogen recombined and bubbled out of the melt pool surface, resulting in volcano-like porous defects at the top surface (white arrows in Figure 9b,d). In a subsequent publication, Kamat et al. [110] reported that reducing the concentration of nitrogen above the melt pool, either by reducing the incident energy density (e.g., by increasing the scan speed) or by diluting the nitrogen flow with argon, eliminated the formation of pores on the top surface. While the dilution of nitrogen with argon was found to be necessary to eliminate pore and crack formation at the top surface, it led to a drastic reduction in nitrogen uptake (e.g., an 11 vol.% dilution of nitrogen in the LSP reduced the nitrogen intake into the melt pool by 70%) due to reduced Marangoni convection in the melt pool [110].

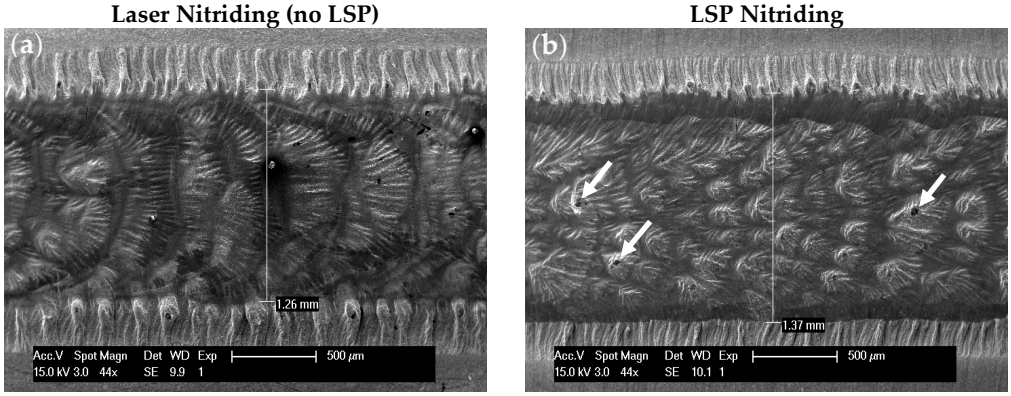

Figure 9. *Cont.*

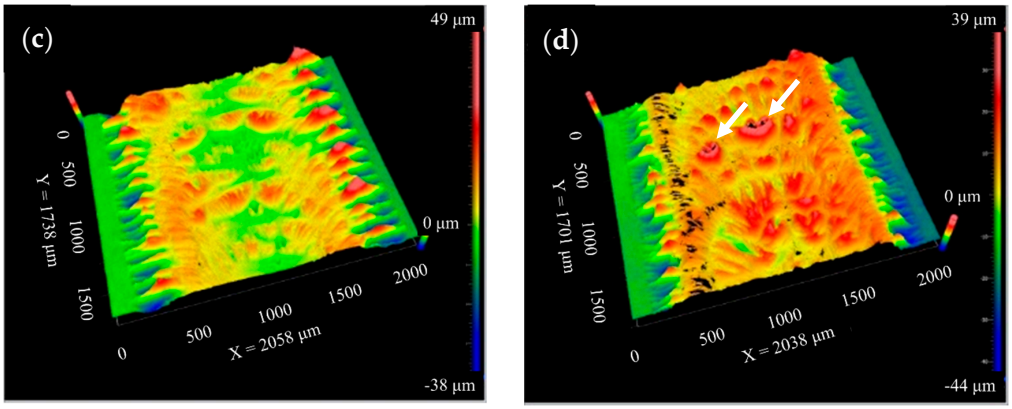

Figure 9. Comparison of LSP and conventional laser nitriding processed under similar conditions: (**a**) and (**c**) scanning electron (SE) micrograph and optical profile of top surface of laser-nitrided trail, respectively; (**b**,**d**) SE micrograph and optical profile of top surface of LSP-nitrided trail, respectively. The pores formed due to nitrogen expulsion from the melt pool in (**b**,**d**) are indicated by white arrows. Reprinted with permission from Ref. [109]. Copyright 2016 John Wiley and Sons.

4.3. Two-Step "LSP Nitriding-Remelting" Process

The nitrogen flow dilution approach described above reduced surface cracking and porosity at the cost of limiting the nitrogen concentration in the melt pool, resulting in microstructures consisting of a thin (~5 µm) TiN layer at the top, with a dendrite-free, martensitic titanium region deeper in the melt pool. Since the thin TiN layer is expected to be removed during a post-processing finishing operation, this microstructure could not sufficiently improve the hardness of titanium and performed poorly in preliminary wear tests. To overcome this reduced control over the microstructure of the nitrided surface layers, Kamat et al. [106] developed a two-step deep-case hardening process (Figure 10a): in the first step, a nitrided layer was deposited on a titanium substrate in the presence of a prestruck, pure-nitrogen LSP, with the laser beam oriented normal to the substrate surface, while in the second step, the nitrided layer from the first step was remelted under a prestruck pure-argon LSP at speeds low enough to partially or fully melt the dendrites. The remelting step recirculated the nitrogen in the melt pool, forming a crack-free and homogenous nitrided layer (Figure 10c) with lower surface roughness (Figure 10e,g); however, this came at the cost of reduced average case hardness of the nitrided layer, since the remelting step diluted the nitrided layer by introducing fresh titanium from the substrate into the nitrogen-rich melt pool. Moreover, the two-step approach offered more control over the microstructure, since the TiN phase fraction (and hence average case hardness) and case depth could be varied by varying the LSP nitriding and/or remelting scan speeds, resulting in microstructures ranging from a two-phase mixture of TiN dendrites embedded in a martensitic α'-Ti matrix to a solid solution of nitrogen in α'-Ti as identified through a combination of energy dispersive spectroscopy (EDS) and X-ray diffraction (XRD). Optimal processing conditions were identified that formed homogeneous and crack-free nitrided layers of case depths up to 800 µm and average case hardness up to 560 HV, showing a 250% hardness increase compared to the untreated CP-Ti substrate (hardness ~160 HV). The two-step LSP nitriding-remelting process developed by Kamat et al. [106] thus represented an improvement over conventional laser nitriding processes due to its ability to form deep, crack-free, homogenous, nitrided cases of any desired thickness on titanium substrates; moreover, due to the oxygen-gettering effect of the LSP [108], the process did not require a controlled nitrogen atmosphere, thus overcoming the issues listed in Table 1.

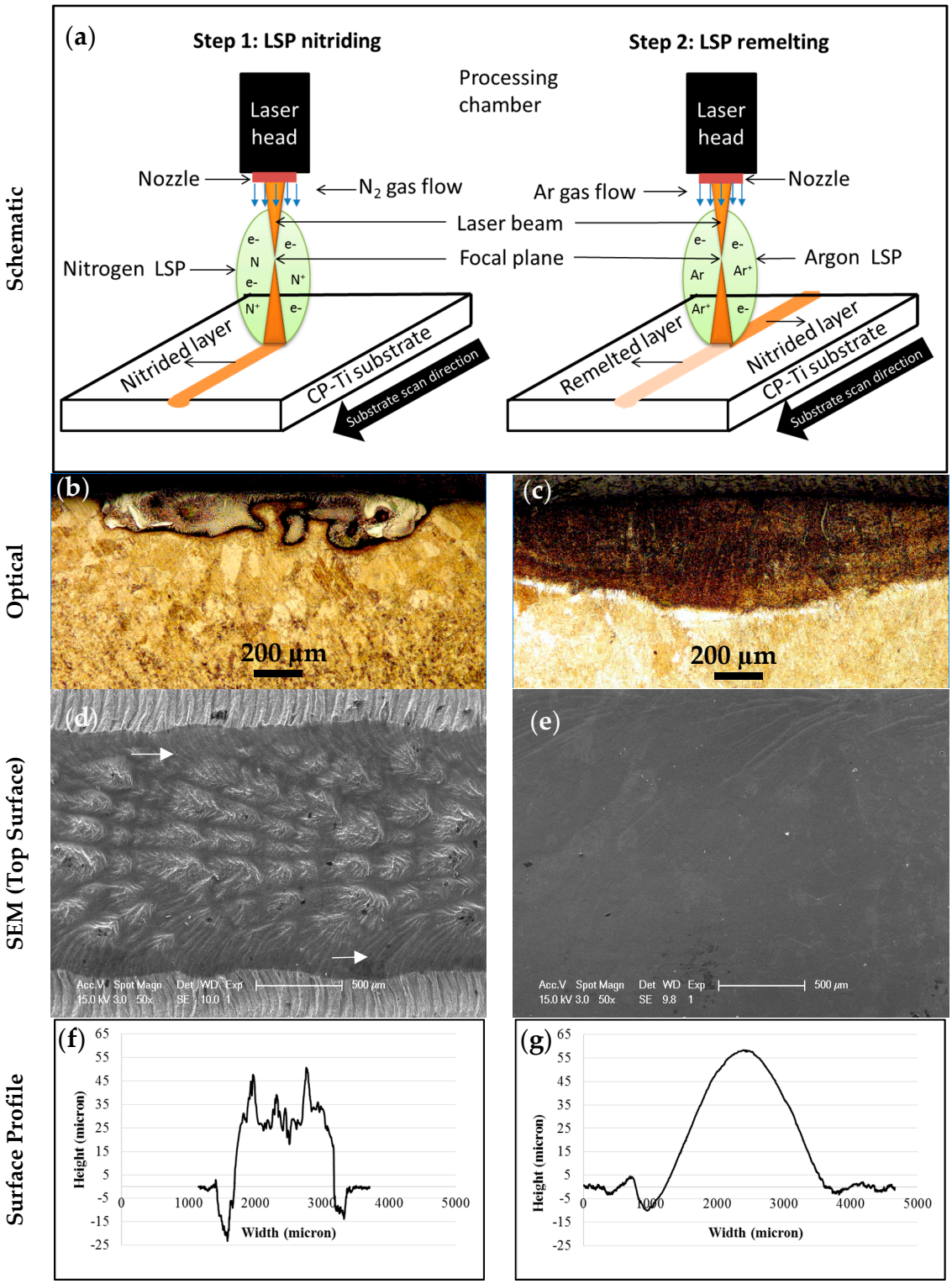

Figure 10. (**a**) Process schematic of two-step LSP nitriding and remelting process; transverse cross-sectional microstructure (**b**) before remelting and (**c**) after remelting; surface microstructure (**d**) before remelting and (**e**) after remelting; surface roughness across the width of the trail (**f**) before remelting and (**g**) after remelting. White arrows in (**d**) point to surface cracks. Reprinted with permission from Ref. [106]. Copyright 2017 Elsevier.

In a subsequent study, Kamat et al. [112] used the two-step processing approach to deposit multiple overlapping trails to perform case hardening of CP-Ti over wider areas. Processing was conducted at different nitriding speeds and the same remelting speed, resulting in nitrided layers of different TiN dendrite volume fractions (Figure 11, where NX refers to a sample nitrided at a speed of *X* mm/s) and, subsequently, different case hardness values; the measured near-surface hardness values of samples N45, N60, and N75 shown in Figure 11 were 870, 621, and 547 HV, respectively. While the N45 sample showed evidence of surface cracking in SE micrographs, samples N60 and N75 were found to be crack-free.

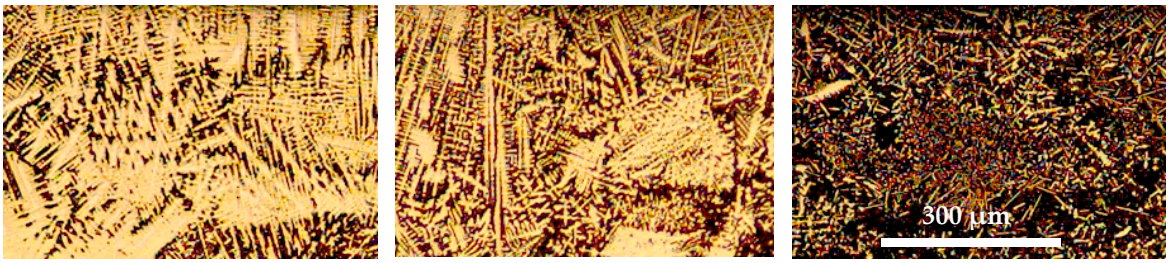

Figure 11. Optical micrographs of transverse cross-section: (**a**) N45 (870 HV, surface cracks), (**b**) N60 (621 HV, no surface cracks), and (**c**) N75 (547 HV, no surface cracks). Reprinted with permission from Ref. [112]. Copyright 2017 Elsevier.

The processed samples were then subjected to reciprocating ball-on-flat wear tests with alumina balls used as the counterbody. Similar to the single trail experiments [106], the remelting step was found to eliminate both the surface microcracks and hot tearing macrocracks penetrating through the depth of the nitrided layer that formed during multi-trail LSP nitriding. Figure 12 provides a summary of the wear test results; the treated samples showed enhanced tribological properties compared to the untreated CP-Ti sample by resisting: (a) oxidative wear of titanium and hence the formation and material transfer of TiO debris to the alumina ball, and (b) plastic deformation from three-body abrasive wear by the TiO debris because of their increased surface hardness, resulting in a wear scar volume reduction in the range of 70%–80% (Figure 12a) on par with a tool steel sample tested under similar conditions. Moreover, it was found that the more homogeneous the microstructure (N75), the lower the friction coefficient recorded during the wear test (Figure 12b); the higher coefficients of friction recorded for the N60 and N45 cases were attributed to hard TiN regions that did not dissolve after the remelting step and caused uneven wear as evident from their respective transverse wear profiles (Figure 12d). Crack-free nitrided layers, with depths up to 600 µm, average case hardness values up to 641 ± 86 HV, and a wear resistance improvement of 70%–80% over that of the untreated titanium substrate, were thus obtained using the LSP nitriding-remelting process.

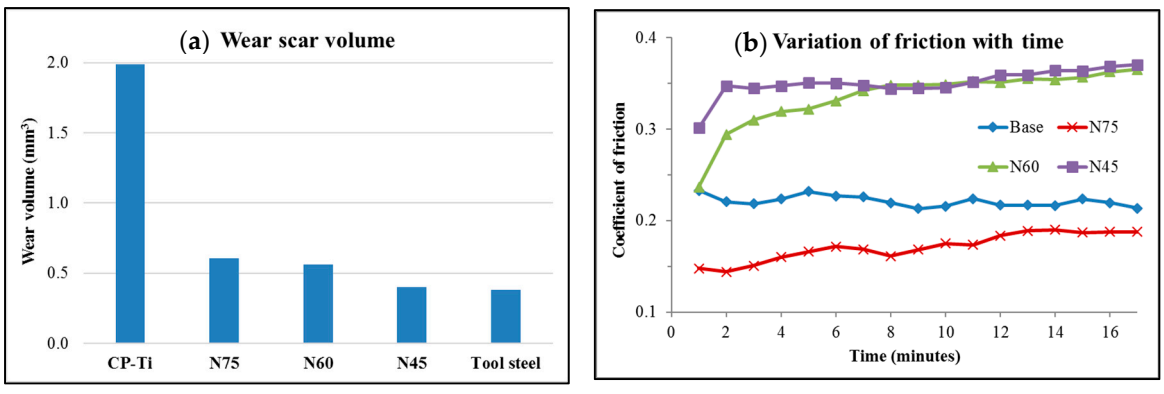

Figure 12. *Cont.*

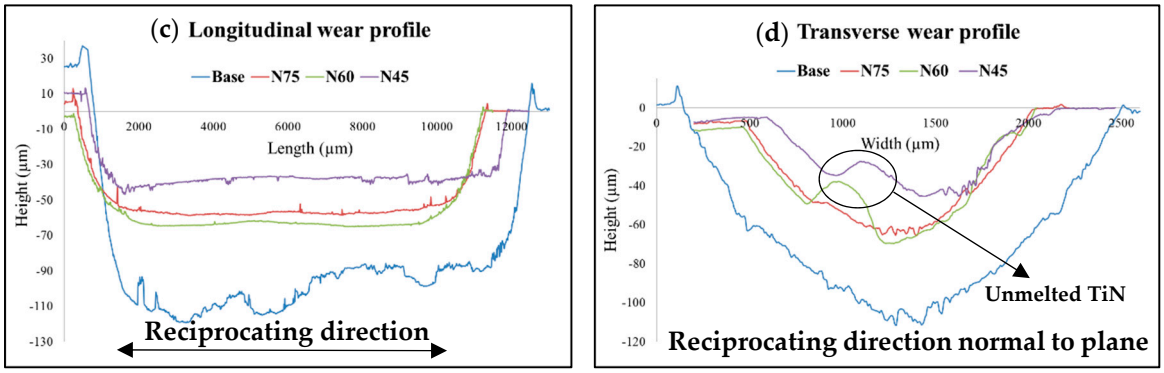

Figure 12. Effect of two-step nitriding-remelting on wear resistance of CP-Ti: (**a**) measured wear scar volumes; (**b**) variation of coefficient of friction over the test duration; wear scar profiles in the (**c**) longitudinal and (**d**) transverse directions. The symbol NX in the figures denotes "nitrided at *X* mm/s speed" i.e., higher the number *X*, lower the nitrogen content and hardness of the nitrided layer. Reprinted with permission from Ref. [112]. Copyright 2017 Elsevier.

5. Summary and Future Directions

In this paper, a critical literature review of the laser nitriding of titanium was presented, with a special emphasis on the role of near-surface plasma. Surface cracking, oxygen contamination of the nitrided layer, surface roughness, and melt pool inhomogeneity were identified as the main challenges in the three decades of research performed on the laser nitriding of titanium. Moreover, the role of plasma was found to be a source of confusion among researchers, with some viewing it as beneficial for enhancing nitrogen intake in the melt pool, while others taking precautions to avoid it to prevent energy attenuation to the substrate due to laser energy absorption by the plasma. Recent research conducted at the Pennsylvania State University studied the role played by near-surface plasma in detail, and revealed that conducting laser nitriding in the presence of a pre-struck, nitrogen-rich, laser-sustained plasma (LSP) in open and uncontrolled atmosphere increased nitrogen intake into the melt pool, minimized surface oxidation, and broadened the incident energy distribution profile without causing any energy attenuation. Furthermore, the pre-struck nitrogen LSP was found to be a potent source of thermal energy and active nitrogen species, capable of forming thick TiN-rich layers on titanium substrates oriented parallel to the laser beam axis i.e., without any direct laser irradiation. The attractive properties of the LSP were further used to develop a novel two-step "LSP nitriding-remelting" case hardening technique which afforded greater control over the microstructure of the nitrided layer than conventional laser nitriding without the need to process in controlled nitrogen atmospheres; the developed process was able to form wide-area, crack-free, homogeneous nitrided layers (up to 600 µm thick and 641 HV hardness) that improved the reciprocating wear resistance of CP-titanium substrates by 70%–80%, thus representing a significant improvement over conventional laser nitriding processes.

Future research directions can focus on a fundamental characterization of the nitrogen LSP using a combination of optical spectroscopy and computational modeling. Insights into the LSP-substrate interaction can be gained by modeling the gas flow and heat transfer occurring during the LSP nitriding process using approaches such as finite element analysis (FEA) or computational fluid dynamics (CFD) to obtain the temperature and nitrogen species (N_2, N, N^+, and so on) concentration as a function of position, similar to prior approaches adopted in the literature to study laser-sustained argon plasmas [100]. The plasma-substrate energy transfer can also be modeled analytically by solving the inverse heat conduction problem, wherein the energy profile of the LSP can be estimated using accurate temperature measurements such as the ones obtained in Figure 8. The "perpendicular" configuration, wherein the laser beam does not directly irradiate the substrate (Figure 6c), also represents an exciting direction to pursue in order to exploit the nitrogen LSP as an energetic source nitrogen species. Another promising direction lies in further development of the two-step LSP nitriding-remelting process; although this process was successful in producing thick, crack-free, and wear-resistant nitrided layers,

further testing (e.g., rolling contact fatigue testing of cylindrical titanium specimens treated using the two-step approach) and process optimization are recommended to evaluate the feasibility of this processing technique as a viable and repeatable case-hardening method for high contact stress applications such as gears and bearings.

Author Contributions: A.M.K. wrote the manuscript; A.E.S., S.M.C., and J.A.T. reviewed and edited it.

Funding: This research was supported by the Office of Naval Research (No. N00014-07-1-0121), the National Science Foundation Graduate Research Fellowship Program, the Penn State Electro-Optics Center, and the P.B. Breneman Chair of Engineering Science and Mechanics at the Pennsylvania State University.

Acknowledgments: The authors acknowledge helpful discussions with Amber Black (Los Alamos National Laboratory) and Abdalla Nassar (Penn State Applied Research Laboratory).

Conflicts of Interest: The authors declare no conflict of interest.

References

1. Donachie, M.J., Jr. *Titanium–A Technical Guide*, 2nd ed.; ASM International: Materials Park, OH, USA, 2000.
2. Boyer, R.R. Titanium for aerospace: Rationale and applications. *Adv. Perform. Mater.* **1995**, *2*, 349–368. [CrossRef]
3. Boyer, R.R. Attributes, characteristics, and applications of titanium and its alloys. *JOM* **2010**, *62*, 21–24. [CrossRef]
4. Long, M.; Rack, H.J. Titanium alloys in total joint replacement–A materials science perspective. *Biomaterials* **1998**, *19*, 1621–1639. [CrossRef]
5. Imam, M.A. The 13th world conference on titanium (Ti-2015). *JOM* **2016**, *68*, 2492–2501. [CrossRef]
6. Ehtemam-Haghighi, S.; Attar, H.; Dargusch, M.S.; Kent, D. Microstructure, phase composition and mechanical properties of new, low cost Ti-Mn-Nb alloys for biomedical applications. *J. Alloy. Compd.* **2019**, *787*, 570–577. [CrossRef]
7. Ehtemam-Haghighi, S.; Cao, G.; Zhang, L.C. Nanoindentation study of mechanical properties of Ti based alloys with Fe and Ta additions. *J. Alloy. Compd.* **2017**, *692*, 892–897. [CrossRef]
8. Li, Y.; Yang, C.; Zhao, H.; Qu, S.; Li, X.; Li, Y. New developments of Ti-based alloys for biomedical applications. *Materials* **2014**, *7*, 1709–1800. [CrossRef]
9. Froes, F.H.; Imam, M.A. Cost affordable developments in titanium technology and applications. *Key Eng. Mater.* **2010**, *436*, 1–11. [CrossRef]
10. Budinski, K.G. Tribological properties of titanium alloys. *Wear* **1991**, *151*, 203–217. [CrossRef]
11. Miller, P.D.; Holladay, J.W. Friction and wear properties of titanium. *Wear* **1958**, *2*, 133–140. [CrossRef]
12. Qu, J.; Blau, P.J.; Watkins, T.R.; Cavin, O.B.; Kulkarni, N.S. Friction and wear of titanium alloys sliding against metal, polymer, and ceramic counterfaces. *Wear* **2005**, *258*, 1348–1356. [CrossRef]
13. Hong, H.; Winer, W.O. A fundamental tribological study of Ti/Al_2O_3 contact in sliding wear. *J. Tribol.* **1989**, *111*, 504–509. [CrossRef]
14. Bhansali, K.J.; Miller, A.E. The role of stacking fault energy on galling and wear behavior. *Wear* **1982**, *75*, 241–252. [CrossRef]
15. Buckley, D.H.; Kuczkowski, T.J.; Johnson, R.L. *Influence of Crystal Structure on the Friction and Wear of Titanium and Titanium Alloys in Vacuum*; National Aeronautics and Space Administration, Lewis Research Center: Cleveland, OH, USA, 1965.
16. Buckley, D.H. The metal-to-metal interface and its effect on adhesion and friction. In *Plenary and Invited Lectures*; Kerker, M., Rowell, R.L., Zettlemoyer, A.C., Eds.; Academic Press: Cambridge, MA, USA, 1977; pp. 37–54.
17. Miyoshi, K.; Buckley, D.H. Correlation of tensile and shear strengths of metals with their friction properties. *ASLE Trans.* **1984**, *27*, 15–23. [CrossRef]
18. Molinari, A.; Straffelini, G.; Tesi, B.; Bacci, T. Dry sliding wear mechanisms of the Ti6Al4V alloy. *Wear* **1997**, *208*, 105–112. [CrossRef]
19. Hutchings, I.M. *Tribology: Friction and Wear of Engineering Materials*, 1st ed.; Butterworth-Heinemann: Oxford, UK, 1992.

20. Bloyce, A.; Morton, P.H.; Bell, T. Surface engineering of titanium and titanium alloys. In *ASM Handbook*; ASM International: Materials Park, OH, USA, 1994; Volume 5, pp. 835–851.
21. Zhecheva, A.; Sha, W.; Malinov, S.; Long, A. Enhancing the microstructure and properties of titanium alloys through nitriding and other surface engineering methods. *Surf. Coat. Technol.* **2005**, *200*, 2192–2207. [CrossRef]
22. Kustas, F.M.; Misra, M.S. Friction and wear of titanium alloys. In *ASM Handbook*; ASM International: Materials Park, OH, USA, 1992; Volume 18, pp. 778–784.
23. Budinski, K.G. *Surface Engineering for Wear Resistance*; Prentice Hall: Englewood Cliffs, NJ, USA, 1988.
24. Bell, T.; Bergmann, H.W.; Lanagan, J.; Morton, P.H.; Staines, A.M. Surface engineering of titanium with nitrogen. *Surf. Eng.* **1986**, *2*, 133–143. [CrossRef]
25. Weng, F.; Chen, C.; Yu, H. Research status of laser cladding on titanium and its alloys: A review. *Mater. Des.* **2014**, *58*, 412–425. [CrossRef]
26. Nazari, K.A.; Rahman Rashid, R.A.; Palanisamy, S.; Xia, K.; Dargusch, M.S. A novel Ti-Fe composite coating deposited using laser cladding of low cost recycled nano-crystalline titanium powder. *Mater. Lett.* **2018**, *229*, 301–304. [CrossRef]
27. Rahman Rashid, R.A.; Palanisamy, S.; Attar, H.; Bermingham, M.; Dargusch, M.S. Metallurgical features of direct laser-deposited Ti6Al4V with trace boron. *J. Manuf. Process.* **2018**, *35*, 651–656. [CrossRef]
28. Aich, S.; Ravi Chandran, K.S. TiB whisker coating on titanium surfaces by solid-state diffusion: Synthesis, microstructure, and mechanical properties. *Metall. Mater. Trans. A* **2002**, *33*, 3489–3498. [CrossRef]
29. Atar, E.; Kayali, E.S.; Cimenoglu, H. Characteristics and wear performance of borided Ti6Al4V alloy. *Surf. Coat. Technol.* **2008**, *202*, 4583–4590. [CrossRef]
30. Kaestner, P.; Olfe, J.; Rie, K.T. Plasma-assisted boriding of pure titanium and TiA16V4. *Surf. Coat. Technol.* **2001**, *142–144*, 248–252. [CrossRef]
31. Zhecheva, A.; Malinov, S.; Sha, W. Titanium alloys after surface gas nitriding. *Surf. Coat. Technol.* **2006**, *201*, 2467–2474. [CrossRef]
32. de Souza, G.B.; Foerster, C.E.; da Silva, S.L.R.; Serbena, F.C.; Lepienski, C.M.; dos Santos, C.A. Hardness and elastic modulus of ion-nitrided titanium obtained by nanoindentation. *Surf. Coat. Technol.* **2005**, *191*, 76–82. [CrossRef]
33. Shibata, H.; Tokaji, K.; Ogawa, T.; Hori, C. The effect of gas nitriding on fatigue behaviour in titanium alloys. *Int. J. Fatigue* **1994**, *16*, 370–376. [CrossRef]
34. Tamura, Y.; Yokoyama, A.; Watari, F.; Kawasaki, T. Surface properties and biocompatibility of nitrided titanium for abrasion resistant implant materials. *Dent. Mater. J.* **2002**, *21*, 355–372. [CrossRef] [PubMed]
35. Bertóti, I.; Mohai, M.; Sullivan, J.L.; Saied, S.O.; Bertoti, I.; Mohai, M.; Sullivan, J.L.; Saied, S.O. Surface characterisation of plasma-nitrided titanium: An XPS study titanium. *Appl. Surf. Sci.* **1995**, *84*, 357–371. [CrossRef]
36. Nolan, D.; Huang, S.W.; Leskovsek, V.; Braun, S. Sliding wear of titanium nitride thin films deposited on Ti–6Al–4V alloy by PVD and plasma nitriding processes. *Surf. Coat. Technol.* **2006**, *200*, 5698–5705. [CrossRef]
37. Yilbaş, B.S.; Şahin, A.Z.; Al-Garni, A.Z.; Said, S.A.M.; Ahmed, Z.; Abdulaleem, B.J.; Sami, M. Plasma nitriding of Ti-6Al-4V alloy to improve some tribological properties. *Surf. Coat. Technol.* **1996**, *80*, 287–292. [CrossRef]
38. Molinari, A.; Straffelini, G.; Tesi, B.; Bacci, T.; Pradelli, G. Effects of load and sliding speed on the tribological behaviour of Ti-6Al-4V plasma nitrided different temperatures. *Wear* **1997**, *203–204*, 447–454. [CrossRef]
39. Muraleedharan, T.M.; Meletis, E.I. Surface modification of pure titanium and Ti-6A1-4V by intensified plasma ion nitriding. *Thin Solid Films* **1992**, *221*, 104–113. [CrossRef]
40. Huang, H.H.; Hsu, C.H.; Pan, S.J.; He, J.L.; Chen, C.C.; Lee, T.L. Corrosion and cell adhesion behavior of TiN-coated and ion-nitrided titanium for dental applications. *Appl. Surf. Sci.* **2005**, *244*, 252–256. [CrossRef]
41. Dong, H.; Li, X.Y. Oxygen boost diffusion for the deep-case hardening of titanium alloys. *Mater. Sci. Eng. A* **2000**, *280*, 303–310. [CrossRef]
42. Bloyce, A.; Qi, P.Y.; Dong, H.; Bell, T. Surface modification of titanium alloys for combined improvements in corrosion and wear resistance. *Surf. Coat. Technol.* **1998**, *107*, 125–132. [CrossRef]
43. Guleryuz, H.; Cimenoglu, H. Surface modification of a Ti-6Al-4V alloy by thermal oxidation. *Surf. Coat. Technol.* **2005**, *192*, 164–170. [CrossRef]
44. Biswas, A.; Dutta Majumdar, J. Surface characterization and mechanical property evaluation of thermally oxidized Ti-6Al-4V. *Mater. Charact.* **2009**, *60*, 513–518. [CrossRef]

45. Borgioli, F.; Galvanetto, E.; Iozzelli, F.; Pradelli, G. Improvement of wear resistance of Ti-6Al-4V alloy by means of thermal oxidation. *Mater. Lett.* **2005**, *59*, 2159–2162. [CrossRef]
46. Conrad, H. Effect of interstitial solutes on the strength and ductility of titanium. *Prog. Mater. Sci.* **1981**, *26*, 123–403. [CrossRef]
47. Wriedt, H.A.; Murray, J.L. The N-Ti (nitrogen-titanium) system. *Bull. Alloy Phase Diagr.* **1987**, *8*, 378–388. [CrossRef]
48. Murray, J.L.; Wriedt, H.A. The O-Ti (Oxygen-Titanium) system. *J. Phase Equilib.* **1987**, *8*, 148–165.
49. Jaffee, R.I. The physical metallurgy of titanium alloys. *Prog. Met. Phys.* **1958**, *7*, 65–163. [CrossRef]
50. Wilson, A.D.; Leyland, A.; Matthews, A. A comparative study of the influence of plasma treatments, PVD coatings and ion implantation on the tribological performance of Ti-6Al-4V. *Surf. Coat. Technol.* **1999**, *114*, 70–80. [CrossRef]
51. Roliński, E. Surface properties of plasma-nitrided titanium alloys. *Mater. Sci. Eng. A* **1989**, *108*, 37–44. [CrossRef]
52. Steen, W.M.; Mazumder, J. Laser welding. In *Laser Material Processing*, 4th ed.; Springer: London, UK, 2010; pp. 199–249.
53. Katayama, S.; Matsunawa, A.; Morimoto, A.; Ishimoto, S.; Arata, Y. Surface hardening of titanium by laser nitriding. *J. Laser Appl.* **1983**, *1983*, 127–134. [CrossRef]
54. Morton, P.H.; Bell, T.; Weisheit, A.; Kroll, J.; Mordike, B.L.; Sagoo, K. Laser gas nitriding of titanium and titanium alloys. *Surf. Modif. Technol.* **1991**, *V*, 593–609.
55. Bell, T.; Morton, P.H.; Bloyce, A. Towards the design of dynamically loaded titanium engineering components. *Mater. Sci. Eng. A* **1994**, *184*, 73–86. [CrossRef]
56. Liu, J.; Luo, Q.; Zou, Z. Laser gas alloying of titanium alloy with nitrogen. *Surf. Coat. Technol.* **1993**, *57*, 191–195. [CrossRef]
57. Kloosterman, A.B.; De Hosson, J.T.M. Microstructural characterization of laser nitrided titanium. *Scr. Metall. Mater.* **1995**, *33*, 567–573. [CrossRef]
58. Mridha, S.; Baker, T.N. Characteristic features of laser-nitrided surfaces of two titanium alloys. *Mater. Sci. Eng. A* **1991**, *142*, 115–124. [CrossRef]
59. Mridha, S.; Baker, T.N. Crack-free hard surfaces produced by laser nitriding of commercial purity titanium. *Mater. Sci. Eng. A* **1994**, *188*, 229–239. [CrossRef]
60. Weerasinghe, V.M.; West, D.R.F.; De Damborenea, J. Laser surface nitriding of titanium and a titanium alloy. *J. Mater. Process. Technol.* **1996**, *58*, 79–86. [CrossRef]
61. Hu, C.; Baker, T.N. The importance of preheat before laser nitriding a Ti–6Al–4V alloy. *Mater. Sci. Eng. A* **1999**, *265*, 268–275. [CrossRef]
62. Xue, L.; Islam, M.; Koul, A.K.; Bibby, M.; Wallace, W. Laser gas nitriding of Ti-6Al-4V Part 1: Optimization of the process. *Adv. Perform. Mater.* **1997**, *4*, 25–47. [CrossRef]
63. Xue, L.; Islam, M.; Koul, A.K.; Bibby, M.; Wallace, W. Laser gas nitriding of Ti-6Al-4V Part 2: Characteristics of nitrided layers. *Adv. Perform. Mater.* **1997**, *4*, 389–408. [CrossRef]
64. Hu, C.; Xin, H.; Watson, L.M.; Baker, T.N. Analysis of the phases developed by laser nitriding Ti6Al4V alloys. *Acta Mater.* **1997**, *45*, 4311–4322. [CrossRef]
65. Xin, H.; Hu, C.; Baker, T.N. Microstructural assessment of laser nitrided Ti-6Al-4V alloy. *J. Mater. Sci.* **2000**, *35*, 3373–3382. [CrossRef]
66. Kaspar, J.; Bretschneider, J.; Jacob, S.; Bonß, S.; Winderlich, B.; Brenner, B. Microstructure, hardness and cavitation erosion behaviour of Ti–6Al–4V laser nitrided under different gas atmospheres. *Surf. Eng.* **2007**, *23*, 99–106. [CrossRef]
67. Nwobu, A.I.P.; Rawlings, R.D.; West, D.R.F. Nitride formation in titanium based substrates during laser surface melting in nitrogen–argon atmospheres. *Acta Mater.* **1999**, *47*, 631–643. [CrossRef]
68. Yerramareddy, S.; Bahadur, S. The effect of laser surface treatments on the tribological behavior of Ti-6Al4V. *Wear* **1992**, *157*, 245–262. [CrossRef]
69. Xin, H.; Mridha, S.; Baker, T.N. The effect of laser surface nitriding with a spinning laser beam on the wear resistance of commercial purity titanium. *J. Mater. Sci.* **1996**, *31*, 22–30. [CrossRef]
70. Man, H.C.; Cui, Z.D.; Yue, T.M.; Cheng, F.T. Cavitation erosion behavior of laser gas nitrided Ti and Ti6Al4V alloy. *Mater. Sci. Eng. A* **2003**, *355*, 167–173. [CrossRef]

71. Ettaqi, S.; Hays, V.; Hantzpergue, J.J.; Saindrenan, G.; Remy, J.C. Mechanical, structural and tribological properties of titanium nitrided by a pulsed laser. *Surf. Coat. Technol.* **1998**, *100–101*, 428–432. [CrossRef]
72. Chen, X.; Wu, G.; Wang, R.; Guo, W.; Yang, J.; Cao, S.; Wang, Y.; Han, W. Laser nitriding of titanium alloy in the atmosphere environment. *Surf. Coat. Technol.* **2007**, *201*, 4843–4846. [CrossRef]
73. Abboud, J.H.; Fidel, A.F.; Benyounis, K.Y. Surface nitriding of Ti–6Al–4V alloy with a high power CO_2 laser. *Opt. Laser Technol.* **2008**, *40*, 405–414. [CrossRef]
74. Chan, C.W.; Lee, S.; Smith, G.C.; Donaghy, C. Fibre laser nitriding of titanium and its alloy in open atmosphere for orthopaedic implant applications: Investigations on surface quality, microstructure and tribological properties. *Surf. Coat. Technol.* **2017**, *309*, 628–640. [CrossRef]
75. Raaif, M.; El-Hossary, F.M.; Negm, N.Z.; Khalil, S.M.; Kolitsch, A.; Höche, D.; Kaspar, J.; Mändl, S.; Schaaf, P. CO_2 laser nitriding of titanium. *J. Phys. D. Appl. Phys.* **2008**, *41*, 085208. [CrossRef]
76. Katahira, K.; Tanida, Y.; Takesue, S.; Komotori, J. Rapid surface nitriding of titanium alloy by a nanosecond fiber laser under atmospheric conditions. *CIRP Ann.* **2018**, *67*, 563–566. [CrossRef]
77. Geetha, M.; Singh, A.K.; Asokamani, R.; Gogia, A.K. Ti based biomaterials, the ultimate choice for orthopaedic implants—A review. *Prog. Mater. Sci.* **2009**, *54*, 397–425. [CrossRef]
78. Geetha, M.; Kamachi Mudali, U.; Pandey, N.D.; Asokamani, R.; Raj, B. Microstructural and corrosion evaluation of laser surface nitrided Ti-13Nb-13Zr alloy. *Surf. Eng.* **2004**, *20*, 68–74. [CrossRef]
79. Vadiraj, A.; Kamaraj, M.; Gnanamoorthy, R. Fretting wear studies on uncoated, plasma nitrided and laser nitrided biomedical titanium alloys. *Mater. Sci. Eng. A* **2007**, *445–446*, 446–453. [CrossRef]
80. Sathish, S.; Geetha, M.; Pandey, N.D.; Richard, C.; Asokamani, R. Studies on the corrosion and wear behavior of the laser nitrided biomedical titanium and its alloys. *Mater. Sci. Eng. C* **2010**, *30*, 376–382. [CrossRef]
81. Zhang, C.H.; Tang, L.W.; Hu, F.; Zhang, S.; Man, H.C. Study on wear and corrosion properties of Ti6Al4V alloy by laser gas nitriding. *Adv. Mater. Res.* **2011**, *299–300*, 188–192. [CrossRef]
82. Majumdar, J.D. Laser gas alloying of Ti-6Al-4V. *Phys. Procedia* **2011**, *12*, 472–477. [CrossRef]
83. Dahotre, S.N.; Vora, H.D.; Rajamure, R.S.; Huang, L.; Banerjee, R.; He, W.; Dahotre, N.B. Laser induced nitrogen enhanced titanium surfaces for improved osseo-integration. *Ann. Biomed. Eng.* **2014**, *42*, 50–61. [CrossRef]
84. Chan, C.W.; Lee, S.; Smith, G.; Sarri, G.; Ng, C.H.; Sharba, A.; Man, H.C. Enhancement of wear and corrosion resistance of beta titanium alloy by laser gas alloying with nitrogen. *Appl. Surf. Sci.* **2016**, *367*, 80–90. [CrossRef]
85. Hussein, M.A.; Yilbas, B.; Kumar, A.M.; Drew, R.; Al-Aqeeli, N. Influence of laser nitriding on the surface and corrosion properties of Ti-20Nb-13Zr alloy in artificial saliva for dental applications. *J. Mater. Eng. Perform.* **2018**, *27*, 4655–4664. [CrossRef]
86. Duraiselvam, M.; Valarmathi, A.; Shariff, S.M.; Padmanabham, G. Laser surface nitrided Ti-6Al-4V for light weight automobile disk brake rotor application. *Wear* **2014**, *309*, 269–274. [CrossRef]
87. da Silva Briguente, L.A.N.; Oñoro, J.; Perpétuo Briguente, F.; Assis Resende, F.; Lidovino dos Reis, J.; Pereira Reis, D.A.; de Oliveira, A.C. The influence of laser nitriding on creep behavior of Ti-4Al-4V alloy with widmanstätten microstructure. *Metals* **2019**, *9*, 236. [CrossRef]
88. Höche, D.; Müller, S.; Rapin, G.; Shinn, M.; Remdt, E.; Gubisch, M.; Schaaf, P. Marangoni convection during free electron laser nitriding of titanium. *Metall. Mater. Trans. B* **2009**, *40*, 497–507. [CrossRef]
89. Höche, D.; Shinn, M.; Müller, S.; Schaaf, P. Diffusion, convection, and solidification in cw-mode free electron laser nitrided titanium. *J. Appl. Phys.* **2009**, *105*, 083503. [CrossRef]
90. Lisiecki, A. Titanium matrix composite Ti/TiN produced by diode laser gas nitriding. *Metals* **2015**, *5*, 54–69. [CrossRef]
91. Kuznetsov, G.V.; Nagornova, T.A. Numerical modeling of high-temperature heat and mass transfer at laser nitriding of titanium. *J. Eng. Thermophys.* **2007**, *16*, 73–77. [CrossRef]
92. Dahotre, S.N.; Vora, H.D.; Pavani, K.; Banerjee, R. An integrated experimental and computational approach to laser surface nitriding of Ti–6Al–4V. *Appl. Surf. Sci.* **2013**, *271*, 141–148. [CrossRef]
93. Xuan, F.Z.; Cao, L.Q.; Wang, Z.; Tu, S.T. Mass transport in laser surface nitriding involving the effect of high temperature gradient: Simulation and experiment. *Comput. Mater. Sci.* **2010**, *49*, 104–111. [CrossRef]
94. Grigoryants, A.G. *Basics of Laser Material Processing*; CRC Press: Boca Raton, FL, USA, 1994.
95. Hügel, H.; Dausinger, F. Interaction phenomena. In *Handbook of the Eurolaser Academy: Volume 2*, 1st ed.; Schuocker, D., Ed.; Springer US: New York, NY, USA, 1998; pp. 1–102.

96. Dahotre, N.B.; Harimkar, S.P. *Laser Fabrication and Machining of Materials*; Springer Science & Business Media: New York, NY, USA, 2008.
97. Thomann, A.L.; Boulmer-Leborgne, C.; Andreazza-Vignolle, C.; Andreazza, P.; Hermann, J.; Blondiaux, G. Metal surface nitriding by laser induced plasma. *J. Appl. Phys.* **1996**, *80*, 4673–4684. [CrossRef]
98. Giren, B.G. Absorption of laser radiation in an optical discharge plasma in a gas mixture stream. *J. Phys. D Appl. Phys.* **1991**, *24*, 1086. [CrossRef]
99. Keefer, D.; Welle, R.; Peters, C. Power absorption in laser-sustained argon plasmas. *AIAA J.* **1986**, *24*, 1663–1669. [CrossRef]
100. Akarapu, R.; Nassar, A.R.; Copley, S.M.; Todd, J.A. Numerical model of a laser-sustained argon plasma. *J. Laser Appl.* **2009**, *21*, 169–175. [CrossRef]
101. Ion, J. *Laser Processing of Engineering Materials: Principles, Procedure and Industrial Application*; Elsevier: Boston, MA, USA, 2005.
102. Höche, D.; Rapin, G.; Schaaf, P. FEM simulation of the laser plasma interaction during laser nitriding of titanium. *Appl. Surf. Sci.* **2007**, *254*, 888–892. [CrossRef]
103. Ohtsu, N.; Saito, W.; Yamane, M. Selectable surface nitridation of titanium using focused pulsed Nd:YAG laser irradiation with nitrogen gas blow. *Surf. Coat. Technol.* **2014**, *246*, 52–56. [CrossRef]
104. Yu, H.; Sun, F. Laser and plasma nitriding of titanium in the atmosphere environment. In Proceedings of the 2009 Symposium on Photonics and Optoelectronics, Wuhan, China, 14–16 August 2009; pp. 1–4.
105. Ohtsu, N.; Saito, W.; Yamane, M. Thickness of titanium nitride layers formed by focused low-powe nitrogen atmospheresr pulsed Nd:YAG laser irradiation in nitrogen atmospheres. *Surf. Coat. Technol.* **2014**, *244*, 57–62. [CrossRef]
106. Kamat, A.M.; Copley, S.M.; Todd, J.A. A two-step laser-sustained plasma nitriding process for deep-case hardening of commercially pure titanium. *Surf. Coat. Technol.* **2017**, *313*, 82–95. [CrossRef]
107. Filip, R. Laser nitriding of the surface layer of Ti6Al4V titanium alloy. *Arch. Mater. Sci. Eng.* **2008**, *30*, 25–28.
108. Nassar, A.R.; Akarapu, R.; Copley, S.M.; Todd, J.A. Investigations of laser-sustained plasma and its role in laser nitriding of titanium. *J. Phys. D Appl. Phys.* **2012**, *45*, 185401. [CrossRef]
109. Kamat, A.M.; Copley, S.M.; Todd, J.A. Effect of CO_2 laser-sustained nitrogen plasma on heat and mass transfer during laser-nitriding of commercially-pure titanium. In *Proceedings of the 13th World Conference on Titanium, San Diego, CA, USA, 16–20 August 2015*; Venkatesh, V., Pilchak, A.L., Eds.; John Wiley & Sons, Inc.: San Diego, CA, USA, 2016; pp. 893–898.
110. Kamat, A.M.; Copley, S.M.; Todd, J.A. Effect of processing parameters on microstructure during laser-sustained plasma (LSP) nitriding of commercially-pure titanium. *Acta Mater.* **2016**, *107*, 72–82. [CrossRef]
111. Black, A.N.; Copley, S.M.; Todd, J.A. A new method for isolating plasma interactions from those of the laser beam during plasma nitriding. *Mater. Charact.* **2017**, *134*, 143–151. [CrossRef]
112. Kamat, A.M.; Segall, A.E.; Copley, S.M.; Todd, J.A. Enhancement of CP-titanum wear resistance using a two-step CO_2 laser-sustained plasma nitriding process. *Surf. Coat. Technol.* **2017**, *325*, 229–238. [CrossRef]
113. Kamat, A.M. A two-step CO_2 Laser-Sustained Plasma Nitriding Process for Deep-Case Hardening of Commercially Pure Titanium. Ph.D. Thesis, Pennsylvania State University, University Park, PA, USA, December 2016.